PVP-Vol. 234, Computer Technology:
Advances and Applications
ASME 1992

THE COUPLING OF FINITE ELEMENTS AND BOUNDARY ELEMENTS FOR SCATTERING FROM FLUID-FILLED STRUCTURES

Gordon C. Everstine and Raymond S.-C. Cheng
Computational Mechanics Division
David Taylor Research Center
Bethesda, Maryland

ABSTRACT

This paper describes a computational capability for computing the acoustic scattering from general, fluid-filled elastic structures. The approach uses finite elements for modeling the structure and boundary elements for modeling both internal and external fluids. The implementation uses NASHUA, a coupled finite element/boundary element capability built around NASTRAN for computing far-field acoustic pressure fields radiated or scattered by arbitrary, submerged, three-dimensional, elastic structures subjected to time-harmonic loadings due to either internal mechanical forces or external incident pressure. The finite element program (NASTRAN) is used to generate the structural finite element model and to perform most of the required matrix operations. After computing surface pressures and normal velocities, far-field pressures are evaluated using an asymptotic form of the Helmholtz exterior integral equation. The proposed numerical approach is validated by comparing the acoustic field scattered from a submerged fluid filled spherical thin shell to that obtained with a series solution, which is also derived in this paper.

INTRODUCTION

Two basic problems in computational structural acoustics are the calculation of (1) the acoustic pressure field radiated by a general submerged three-dimensional elastic structure subjected to internal time-harmonic loads, and (2) the acoustic pressure scattered by such a structure subjected to an incident time-harmonic wavetrain. The most common, as well as the most accurate, approach for solving these problems at low frequencies is to couple a finite element model of the structure with a boundary element model of the surrounding fluid [1-12]. This is the approach taken by NASHUA, which is a boundary element program built around NASTRAN, a widely-used finite element computer program for structural dynamics.

Several previous papers [6,7,9,10] described the basic formulation and development for acoustic radiation and scattering from evacuated structures. Here we describe the extension of this capability for modeling submerged structures which are fluid-filled. Internal fluid can occur because the structure is free-flooded or contains fluid-filled tanks. It is possible to model the interior fluid with finite elements [13-23], but three-dimensional models with large numbers of fluid degrees of freedom might result. An attractive alternative to the fluid finite element model is to represent the contained fluid using a boundary element approach. In principle, any computer program capable of generating the appropriate boundary element matrices for an exterior fluid is also capable of generating such matrices for interior fluids.

THEORETICAL APPROACH

The basic theoretical development for the NASHUA radiation and scattering approach for evacuated structures has been presented in detail previously [6,7,9,10]. For completeness, this paper summarizes that approach and describes the modifications necessary to model the interior fluid with boundary elements in the same procedure. There is no requirement that the properties of the interior and exterior fluids be the same.

The Surface Solution for Evacuated Structures

Consider any submerged three-dimensional, evacuated elastic structure subjected to either internal time-harmonic loads or an external time-harmonic incident wavetrain. If the structure is modeled with finite elements, the resulting matrix equation of motion can be written as

$$Zv = F - GAp, \tag{1}$$

where matrix Z (of dimension s x s) is the structural impedance, vector v (s x r) is the complex velocity amplitude for all structural DOF (wet and dry) using the coordinate systems selected by the user, vector F (s x r) is the complex amplitude of the mechanical forces applied to the structure, matrix G (s x f) is the rectangular transformation of direction cosines to transform a vector of outward normal forces at the wet points to a vector of forces at all points in the coordinate systems selected by the user, matrix A (f x f) is the diagonal area matrix for the wet surface, and vector p (f x r) is the complex amplitude of pressures (incident + scattered) applied at the wet grid points. In this equation, the time dependence $\exp(i\omega t)$ has been suppressed. In the above dimensions, s denotes the total number of independent structural DOF (wet and dry), f denotes the number of fluid DOF (wet points), and r denotes the number of load cases. In general, the surface areas, the normals, and the transformation matrix G are obtained from the finite element calculation of the load vector resulting from an outwardly directly static unit pressure load on the structure's wet surface.

In Eq. 1, the structural impedance matrix Z, which converts velocity to force, is given by

$$Z = (-\omega^2 M + i\omega B + K)/(i\omega), \tag{2}$$

where M, B, and K are the structural mass, viscous damping, and stiffness matrices, respectively, and ω is the circular frequency of excitation. For structures with a nonzero loss factor, K is complex. In addition, K can include the geometric stiffness effects of hydrostatic pressure, if any [9]. A standard finite element model of the structure

supplies the matrices K, M, and B.

For the exterior fluid domain, the fluid pressure p satisfies the Helmholtz differential equation

$$\nabla^2 p + k^2 p = 0, \tag{3}$$

where $k = \omega/c$ is the acoustic wave number, and c is the fluid sound speed. Equivalently, for the exterior fluid, p is the solution of the Helmholtz integral equations [3]

$$\int_S p(\mathbf{x}) \frac{\partial D(\mathbf{r})}{\partial n} dS - \int_S q(\mathbf{x}) D(\mathbf{r}) dS = \begin{cases} p(\mathbf{x}')/2 - p_I, & \mathbf{x}' \text{ on S,} \\ p(\mathbf{x}') - p_I, & \mathbf{x}' \text{ in E,} \\ -p_I, & \mathbf{x}' \text{ in I,} \end{cases} \tag{4}$$

where S, E, and I denote the surface, exterior, and interior domains, respectively, p_I is the incident free-field pressure (if any), r is the distance from $\mathbf{x}$ to $\mathbf{x}'$ (Fig. 1), D is the free-space Green's function

$$D(r) = \frac{e^{-ikr}}{4\pi r}, \tag{5}$$

$$q = \frac{\partial p}{\partial n} = -i\omega\rho v_n, \tag{6}$$

ρ is the fluid mass density, and v_n is the outward normal velocity on S. As shown in Fig. 1, $\mathbf{x}$ in Eq. 4 is the position vector for a typical point P_j on the surface S, $\mathbf{x}'$ is the position vector for the point P_i on the surface or in the exterior field, the vector $\mathbf{r} = \mathbf{x}' - \mathbf{x}$, and $\mathbf{n}$ is the unit outward normal at P_j. We denote the lengths of the vectors $\mathbf{x}$, $\mathbf{x}'$, and $\mathbf{r}$ by x, x', and r, respectively. The normal derivative of the Green's function D is [6,10]

$$\frac{\partial D(r)}{\partial n} = \frac{e^{-ikr}}{4\pi r}\left(ik + \frac{1}{r}\right)\cos\beta, \tag{7}$$

where β is the angle between the normal $\mathbf{n}$ and the vector $\mathbf{r}$, as shown in Fig. 1.

All three integral equations in Eq. 4 are needed for exterior fluids. The surface equation provides the fluid impedance at the fluid-structure interface. Since the surface equation exhibits non-uniqueness at certain

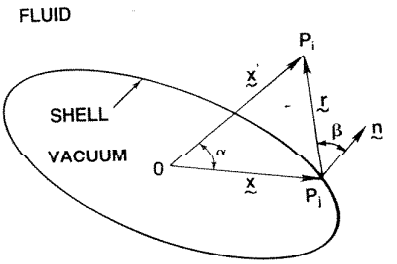

Fig. 1. Notation for Helmholtz Integral Equation

discrete characteristic frequencies [24], the interior equation is used to provide additional constraint equations which ensure the required uniqueness. The exterior equation is used to compute the exterior pressure field once the surface solution (which includes the fluid pressure and its gradient) is known.

The substitution of Eqs. 6 and 7 into the surface equation (4) yields

$$\frac{p(\mathbf{x}')}{2} - \int_S p(\mathbf{x}) \frac{e^{-ikr}}{4\pi r}\left(ik + \frac{1}{r}\right)\cos\beta\, dS = i\omega\rho \int_S v_n(\mathbf{x}) \frac{e^{-ikr}}{4\pi r} dS + p_I, \quad \mathbf{x}' \text{ on S.} \tag{8}$$

This integral equation relates the pressure p and normal velocity v_n on S. If the integrals in Eq. 8 are discretized for numerical computation [6], we obtain the matrix equation (for the exterior fluid)

$$Ep = Cv_n + p_I, \tag{9}$$

where vector p (of dimension f x r) is the vector of complex amplitudes of the pressure on the structure's wet surface, matrices E and C (both f x f) are fully-populated, complex, nonsymmetric, and frequency-dependent, and vector p_I (f x r) is the complex amplitude of the incident pressure vector. The number of unknowns in this system is f, the number of wet points on the fluid-structure interface.

The normal velocity vector v_n in Eq. 9 is related to the full velocity vector v by the same rectangular transformation matrix G:

$$v_n = G^T v, \tag{10}$$

where T denotes the matrix transpose. If velocities v and v_n are eliminated from Eqs. 1, 9, and 10, the resulting equation for the coupled fluid-structure system is

$$(E + CG^TZ^{-1}GA)\, p = CG^TZ^{-1}F + p_I. \tag{11}$$

This equation is solved for the surface pressures p, since the rest of the equation depends only on the geometry, the material properties, and the frequency. Since the two right-hand side terms in Eq. 11 correspond to mechanical and incident loadings, only one of the two terms would ordinarily be present for a given case. The details of the incident pressure vector p_I for scattering problems were presented previously [7] and will not be repeated here.

The velocity vector v for all structural DOF is recovered by solving Eq. 1 for v:

$$v = Z^{-1}F - Z^{-1}GAp. \tag{12}$$

The surface normal velocity vector v_n is recovered by substituting this solution for v into Eq. 10.

Modeling Interior Fluid

The theoretical development presented in the preceding section can be modified slightly to account also for an interior fluid. The wave equation, Eq. 3, applies also to interior fluids. Although all three integral equations in Eq. 4 are generally needed for exterior fluids, only the surface equation is needed to represent the surface impedance of interior fluids. Eq. 4a also applies to interior fluids if the incident pressure p_I is set to zero, and the normal vector $\mathbf{n}$ is negated. That is, the surface integral equation applies to both exterior and interior fluids so long as the unit normal is always directed from the structure into the fluid.

A matrix equation similar to Eq. 9 is therefore obtained for the interior fluid except that the incident pressure p_I is zero. The fluid matrices E and C are different for exterior and interior domains (even if the separating surface S has infinitesimal thickness) because the normals are of opposite sign.

Two-Fluid Formulation

Denote the exterior fluid as Fluid 1 and the interior fluid as Fluid 2, and use the subscripts 1 and 2 to refer to these two domains. Also define new pressure and normal velocity unknowns p and v_n which include the solutions for both fluid domains:

$$p = \begin{Bmatrix} p_1 \\ p_2 \end{Bmatrix}, \quad v_n = \begin{Bmatrix} v_{n1} \\ v_{n2} \end{Bmatrix}. \tag{13}$$

Since there is no direct fluid coupling between the interior and exterior fluids, and the incident pressure vanishes in the interior domain, Eqs. 1, 9, 10, and 11 apply also to the two-fluid problem if the new definitions in Eq. 13 are used, and the matrices A, G, E, C, and p_I are re-defined as

$$A = \begin{bmatrix} A_1 & 0 \\ 0 & A_2 \end{bmatrix}, \quad G = \begin{bmatrix} G_1 & G_2 \end{bmatrix}, \quad E = \begin{bmatrix} E_1 & 0 \\ 0 & E_2 \end{bmatrix}, \quad C = \begin{bmatrix} C_1 & 0 \\ 0 & C_2 \end{bmatrix}, \quad p_I = \begin{Bmatrix} p_{I1} \\ 0 \end{Bmatrix}. \tag{14}$$

The principle benefit of formulating the two-fluid problem in this way is that the required modifications to extend the procedure to three or more independent fluid domains is now clear.

The Far-Field Calculation

With the solution for the pressures and velocities on the surface, the exterior Helmholtz integral equation, Eq. 4b, can be integrated to obtain the radiated (or scattered) pressure at any desired location $\mathbf{x}'$ in the exterior field. We first substitute Eqs. 5 - 7 into Eq. 4b to obtain

$$p(\mathbf{x}') = \int_S [i\omega\rho v_n(\mathbf{x}) + (ik + \frac{1}{r})p(\mathbf{x}) \cos\beta] \frac{e^{ikr}}{4\pi r} dS, \quad \mathbf{x}' \text{ in E.} \quad (15)$$

In applications, however, the field pressures generally of interest are in the far-field, so we use instead the asymptotic form of Eq. 15 [6,10]:

$$p(\mathbf{x}') = \frac{ike^{-ikx'}}{4\pi x'} \int_S [\rho c v_n(\mathbf{x}) + p(\mathbf{x}) \cos\beta] e^{ikx \cos\alpha} dS,$$

$$\mathbf{x}' \text{ in E}, \quad x' \gg d, \quad (16)$$

where d is a characteristic dimension of the structure, and α is the angle between the vectors $\mathbf{x}$ and $\mathbf{x}'$ (Fig. 1). For far-field points, $\cos\beta$ is computed using the asymptotic approximation

$$\cos\beta \rightarrow \mathbf{n} \cdot \frac{\mathbf{x}'}{x'} . \quad (17)$$

For both Eqs. 15 and 16, numerical quadrature is used.

OVERVIEW OF SOLUTION PROCEDURE

The solution procedure uses the finite element program NASTRAN to generate the matrices K, M, B, and F and to generate sufficient geometry information so that the matrices E, C, G, A, and p_I can be computed by a separate program. Then, NASTRAN's matrix routines are used to form the matrices appearing in Eq. 11, which is solved for the pressures p (in both fluid domains) using the block solver OCSOLV [25]. Next, NASTRAN matrix operations are used to recover the surface normal velocities v_n and the vector v of velocities at all structural DOF. This step completes the surface solution. Then, with the pressures and velocities on the (exterior) surface, the asymptotic (far-field) form of the Helmholtz exterior integral equation is integrated to compute the far field radiated pressures. Various tables and graphical displays are generated.

The overall setup of the solution procedure is organized into four steps. In Step 1, a separate finite element structural model is prepared and run for each unique set of symmetry constraints and each fluid region. Since, for general three-dimensional analysis, up to three planes of reflective symmetry are allowed, there would be one, two, four, or eight such runs for each fluid region. Since the purpose of this step is to generate a file containing geometry information and a checkpoint file for subsequent use in the other steps, the only difference between the two runs associated with a given symmetry case is the specification of the outwardly directed unit pressure load which defines the wet surface for a given fluid region.

For each symmetry case and drive frequency, several programs are run sequentially to form Step 2. For each fluid region, the fluid matrix generation program reads the geometry file generated by NASTRAN in Step 1 and, using the Helmholtz surface and interior integral equations, generates the fluid matrices E_1, E_2, C_1, and C_2, the area matrices A_1 and A_2, the structure-fluid transformation matrices G_1 and G_2, the incident pressure vector p_{I1}, and a geometry file to be used later by the far-field integration routine in Step 3. In addition, a partitioning vector is generated to facilitate the merging and partitioning of the various matrices associated with the two fluid domains.

The two fluid matrix generation jobs in Step 2 are followed by a NASTRAN job which takes the structural matrices K, M, B, and F from Step 1 and the fluid matrices and forms the matrices in Eq. 11, where the definitions in Eq. 14 apply. Eq. 11 is then solved for the surface pressure vector p by program OCSOLV, which is a general out-of-core block solver designed specifically for large, full, complex, nonsymmetric systems of linear, algebraic equations. NASTRAN is then re-entered in Step 2 with p so that the velocities v and v_n can be recovered using general matrix operations. The surface pressures, normal velocities, and complete set of displacements are then reformatted, sorted, and merged into a single file for each symmetry case. Recall that there are one, two, four, or eight possible symmetry cases.

Steps 1 and 2 are repeated for each symmetry case. After all symmetry cases have been completed and merged, the symmetry cases are combined and integrated to generate the pressures in the field. The far-field pressure solution is obtained by integrating the surface pressures and velocities using the asymptotic (far-field) form of the exterior Helmholtz integral equation, Eq. 16. Output consists of both tables and files suitable for various types of plotting.

The remaining steps in the procedure are for graphical display, including deformed structural plots of the frequency response, animations [26], X-Y plots, and polar plots.

NUMERICAL EXAMPLE

Here we illustrate and validate the two-fluid boundary element formulation developed above by solving the problem of acoustic scattering from a submerged fluid-filled spherical thin shell. The incident loading is a time-harmonic planar wavetrain, as shown in Fig. 2. The specific problem solved has the following characteristics:

shell mean radius (a)	5 m
shell thickness (h)	0.15 m
shell Young's modulus (E)	2.07×10^{11} N/m^2
shell Poisson's ratio (ν)	0.3
shell density (ρ_s)	7669 kg/m^3
shell loss factor (η)	0.01
fluid density (ρ)	1000 kg/m^3
fluid sound speed (c)	1524 m/s

The same fluid is used for both the exterior and interior fluid domains. The solution of this problem exhibits rotational symmetry about the spherical axis parallel to the direction of wave propagation. The benchmark solution to which the numerical results will be compared is a series solution, the derivation of which is summarized in the next section.

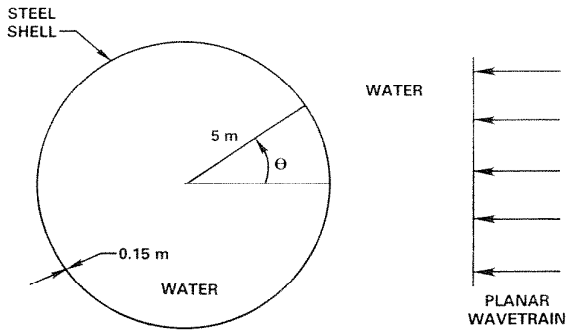

Fig. 2. Plane Wave Scattering from a Fluid-Filled Spherical Shell

Series Solution

The series solution for scattering from a submerged evacuated spherical thin shell was presented by Junger and Feit [27]. Here we summarize that solution and indicate the modification necessary to include the addition of an interior fluid which fills the spherical volume.

In general, the series solution for plane wave scattering from a submerged, evacuated, spherical thin shell involves computing the impedances of the shell and exterior fluid, the scattered field due to rigid body effects, and the radiated field due to elastic (vibrational) effects. The shell impedance (the ratio of pressure to normal velocity) for the nth axisymmetric shell mode is

$$Z_n = -\frac{i\rho_s c_p}{\Omega} \frac{h}{a} \frac{[\Omega^2-(\Omega_n^{(1)})^2][\Omega^2-(\Omega_n^{(2)})^2]}{[\Omega^2-(1+\beta^2)(\nu+\lambda_n-1]}, \quad (18)$$

where ρ_s is the structural mass density, $c_p = \sqrt{E/[\rho_s(1-\nu^2)]}$, E is Young's modulus, ν is Poisson's ratio, $\Omega = \omega a/c_p$ is the dimensionless frequency, h is the shell thickness, a is the shell mean radius,

$\beta = h/(a\sqrt{12})$, and $\lambda_n = n(n+1)$. The quantities $\Omega_n^{(1)}$ and $\Omega_n^{(2)}$ are the upper and lower shell resonance dimensionless frequencies, respectively. They are the solutions of the characteristic equation

$$\Omega^4 - [1+3\nu+\lambda_n-\beta^2(1-\nu-\lambda_n^2-\nu\lambda_n]\,\Omega^2 + (\lambda_n-2)(1-\nu^2)+\beta^2[\lambda_n{}^3-4\lambda_n{}^2+\lambda(5-\nu^2)-2(1-\nu^2)] = 0. \quad (19)$$

The impedance of the exterior fluid, found by using the Green's function and identity for the exterior fluid, is

$$z_n = i\rho c\frac{h_n(ka)}{h'_n(ka)}, \quad (20)$$

where h_n is the Bessel's function of the third kind of order n.

Thus, Junger and Feit showed that the far-field scattered pressure is

$$p(R,\theta) = -\frac{ie^{ikR}p_o}{kR}\sum_{n=0}\frac{(2n+1)P_n(\cos\theta)}{h'_n(ka)} \times \left[j'_n(ka)-\frac{\rho c}{(Z_n+z_n)(ka)^2h'_n(ka)}\right], \quad R>>a, \quad (21)$$

where R is the distance to the field point, θ is the angle from the z-axis, p_o is the incident pressure, P_n is the Legendre polynomial of order n, and j_n is the Bessel's function of the first kind of order n. The two terms in the bracketed expression correspond to rigid body and radiated effects, respectively.

The above expression for the pressure scattered from an evacuated shell can be extended to include the effects of the interior fluid merely by replacing the exterior fluid impedance z_n in Eq. 21 with the sum of the fluid impedances for the exterior and interior fluids. It can be shown, by using the Green's function and identity for the interior domain, that the interior impedance, denoted ζ_n, is given by

$$\zeta_n = -i\rho c\frac{j_n(ka)}{j'_n(ka)}. \quad (22)$$

We note the resemblance between Eqs. 20 and 22 for the exterior and interior domains, respectively.

The above analysis was implemented in a computer program called SCATSPHERE2 [28].

Numerical Solution

A finite element model of the spherical shell was prepared using 40 axisymmetric conical shell elements spanning the 180 degrees between the two poles of the sphere. Due to the axisymmetry of the incident pressure loading, only the N = 0 harmonic was required. Since all structural points are in contact with both interior and exterior fluids, the resulting model therefore had 205 independent structural degrees of freedom (DOF) and 41 fluid DOF for each of the two fluid domains. System matrices for the exterior fluid were also augmented by the addition of four constraint equations associated with interior Chief points to ensure uniqueness of the integral representation at the upper frequencies. The nondimensional frequency range $0<ka<5$ was swept using a frequency increment of about ka = 0.05 with the numerical solution and ka = 0.005 with the series solution. Since the series solution is converged, we treat it as the "exact" solution for this problem.

The comparison between the computed and exact solutions is presented is Figs. 3 and 4, which plot the frequency response of the nondimensional scattered pressure $pr/(p_o a)$, where p is the far-field scattered pressure at distance r from the origin, p_o is the incident pressure, and a is the mean radius of the spherical shell. These two figures show very good agreement between the two scattering solutions in the backward (θ = 0) and forward (θ = 180 degrees) directions. In fact, the computed and series solutions are virtually indistinguishable from each other.

DISCUSSION

A very general computational capability has been described for predicting the sound pressure field radiated or scattered by arbitrary, submerged, fluid-filled, three-dimensional elastic structures subjected to time-harmonic loads. The structure is modeled with NASTRAN (in all the generality that NASTRAN allows) in combination with boundary element models of both interior and exterior fluid domains. Sufficient automation is provided so that, for many structures of practical interest, an existing structural model can be adapted for acoustic analysis within a few hours.

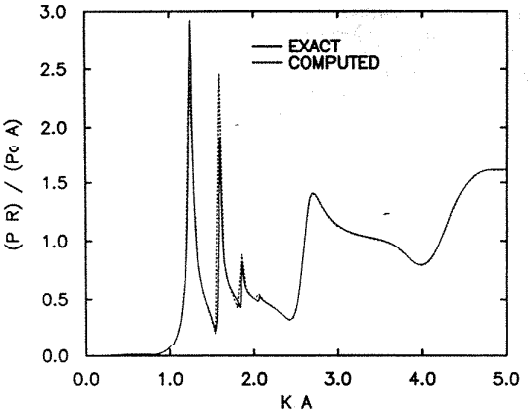

Fig. 3. Forward Scattering from a Fluid-Filled Spherical Shell

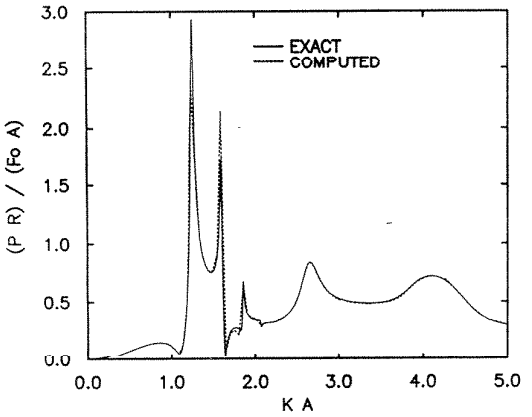

Fig. 4. Backward Scattering from a Fluid-Filled Spherical Shell

One of the many benefits of having the acoustic analysis linked with NASTRAN is the ability to integrate the acoustic analysis of a structure with other dynamic analyses. Thus the same finite element model can be used for modal analysis, frequency response analysis, linear shock analysis, and underwater acoustic analysis. In addition, many of the pre- and postprocessors developed for use with NASTRAN become available for acoustic analysis as well.

REFERENCES

1. L.H. Chen and D.G. Schweikert, "Sound Radiation from an Arbitrary Body," **J. Acoust. Soc. Amer.**, Vol. 35, No. 10, pp. 1626-1632 (1963).
2. J.J. Engblom and R.B. Nelson, "Consistent Formulation of Sound Radiation from Arbitrary Structure," **J. Appl. Mech.**, Vol. 42, pp. 295-300 (1975).
3. D.T. Wilton, "Acoustic Radiation and Scattering from Elastic Structures," **Int. J. Num. Meth. in Engrg.**, Vol. 13, pp. 123-138 (1978).
4. J.S. Patel, "Radiation and Scattering from an Arbitrary Elastic Structure Using Consistent Fluid Structure Formulation," **Comput. Struct.**, Vol. 9, pp. 287-291 (1978).

5. I.C. Mathews, "Numerical Techniques for Three-Dimensional Steady-State Fluid-Structure Interaction," **J. Acoust. Soc. Amer.**, Vol. 79, pp. 1317-1325 (1986).

6. G.C. Everstine, F.M. Henderson, E.A. Schroeder, and R.R. Lipman, "A General Low Frequency Acoustic Radiation Capability for NASTRAN," in **Fourteenth NASTRAN Users' Colloquium**, NASA CP-2419, National Aeronautics and Space Administration, Washington, DC, pp. 293-310 (1986).

7. G.C. Everstine, F.M. Henderson, and L.S. Schuetz, "Coupled NASTRAN/Boundary Element Formulation for Acoustic Scattering," in **Fifteenth NASTRAN Users' Colloquium**, NASA CP-2481, National Aeronautics and Space Administration, Washington, DC, pp. 250-265 (1987).

8. A.F. Seybert, T.W. Wu, and X.F. Wu, "Radiation and Scattering of Acoustic Waves from Elastic Solids and Shells Using the Boundary Element Method," **J. Acoust. Soc. Amer.**, Vol. 84, pp. 1906-1912 (1988).

9. G.C. Everstine, "Treatment of Static Preload Effects in Acoustic Radiation and Scattering," in **Sixteenth NASTRAN Users' Colloquium**, NASA CP-2505, National Aeronautics and Space Administration, Washington, DC, pp. 138-152 (1988).

10. G.C. Everstine and F.M. Henderson, "Coupled Finite Element/Boundary Element Approach for Fluid-Structure Interaction," **J. Acoust. Soc. Amer.**, Vol. 87, No. 5, pp. 1938-1947 (1990).

11. G.C. Everstine, "Prediction of Low Frequency Vibrational Frequencies of Submerged Structures," **J. Vibration and Acoustics**, Vol. 13, No. 2, pp. 187-191 (1991).

12. J.H. Kane, S. Mao, and G.C. Everstine, "A Boundary Element Formulation for Acoustic Shape Sensitivity Analysis," **J. Acoust. Soc. Amer.**, Vol. 90, No. 1, pp. 561-573 (1991).

13. O.C. Zienkiewicz and R.E. Newton, "Coupled Vibrations of a Structure Submerged in a Compressible Fluid," **Proc. Internat Symp. on Finite Element Techniques**, Stuttgart, pp. 359-379 (1969).

14. A. Craggs, "The Transient Response of a Coupled Plate-Acoustic System Using Plate and Acoustic Finite Elements," **J. Sound and Vibration**, Vol. 15, No. 4, pp. 509-528 (1971).

15. A.J. Kalinowski, "Fluid Structure Interaction," **Shock and Vibration Computer Programs: Reviews and Summaries**, SVM-10, ed. by W. Pilkey and B. Pilkey, The Shock and Vibration Information Center, Naval Research Laboratory, Washington, DC, pp. 405-452 (1975).

16. L. Kiefling and G.C. Feng, "Fluid-Structure Finite Element Vibrational Analysis," **AIAA J.**, Vol. 14, No. 2, pp. 199-203 (1976).

17. A.J. Kalinowski, "Transmission of Shock Waves into Submerged Fluid Filled Vessels," **Fluid Structure Interaction Phenomena in Pressure Vessel and Piping Systems**, PVP-PB-026, ed. by M.K. Au-Yang and S.J. Brown, Jr., The American Society of Mechanical Engineers, New York, pp. 83-105 (1977).

18. O.C. Zienkiewicz and P. Bettess, "Fluid-Structure Dynamic Interaction and Wave Forces: An Introduction to Numerical Treatment," **Int. J. Num. Meth. in Engrg.**, Vol. 13, No. 1, pp. 1-6 (1978).

19. M.A. Hamdi and Y. Ousset, "A Displacement Method for the Analysis of Vibrations of Coupled Fluid-Structure Systems," **Int. J. Num. Meth. in Engrg.**, Vol. 13, No. 1, pp. 139-150 (1978).

20. G.C. Everstine, "Structural Analogies for Scalar Field Problems," **Int. J. Num. Meth. in Engrg.**, Vol 17, pp. 471 476 (1981).

21. G.C. Everstine, "A Symmetric Potential Formulation for Fluid-Structure Interaction," **J. Sound and Vibration**, Vol. 79, pp. 157-160 (1981).

22. A.J. Kalinowski and C.W. Nebelung, "Media-Structure Interaction Computations Employing Frequency-Dependent Mesh Size with the Finite Element Method," **Shock Vib. Bull.**, Vol 51, No. 1, pp. 173-193 (1981).

23. G.C. Everstine, "Structural-Acoustic Finite Element Analysis, with Application to Scattering," in **Proc. 6th Invitational Symposium on the Unification of Finite Elements, Finite Differences, and Calculus of Variations**, edited by H. Kardestuncer, Univ. of Connecticut, Storrs, Connecticut, pp. 101-122 (1982).

24. H.A. Schenck, "Improved Integral Formulation for Acoustic Radiation Problems," **J. Acoust. Soc. of Amer.**, Vol. 44, pp. 41-58 (1968).

25. E.A. Schroeder, "A New Block Solver for Large, Full, Unsymmetric, Complex Systems of Linear Algebraic Equations," Report 88/003, David Taylor Research Center, Bethesda, Maryland (1988).

26. R.R. Lipman, "Computer Animation of Modal and Transient Vibrations," in **Fifteenth NASTRAN Users' Colloquium**, NASA CP-2481, National Aeronautics and Space Administration, Washington, DC, pp. 88-97 (1987).

27. M.C. Junger and D. Feit, **Sound, Structures, and Their Interaction**, Second Edition, The MIT Press, Cambridge, Massachusetts (1986).

28. R.S. Cheng and F.M. Henderson, "SCATSPHERE2 -- A Computation for the Plane Wave Scattering from a Submerged, Elastic, Spherical, Evacuated or Fluid-Filled, Thin Shell," Report 90/029, David Taylor Research Center, Bethesda, MD (1990).